SF2A 2025
A. Siebert, K. Baillié, M. Béthermin, F. Cantalloube, E. Josselin, N. Lagarde, J. Malzac, J. Richard, L. Selliez, O. Venot (eds)

UNRAVELING THE NON-EQUILIBRIUM CHEMISTRY OF THE TEMPERATE SUB-NEPTUNE K2-18 B

A. Y. Jaziri[1,2], O. Sohier[1], O. Venot[3] and N. Carrasco[1,4]

Abstract. The detection and characterization of temperate, Earth-like exoplanets remain challenging, but M-dwarf systems provide favorable conditions for atmospheric studies of sub-Neptunes. We investigate the atmosphere of K2-18 b, a temperate sub-Neptune in the habitable zone of an M-dwarf, using JWST data combined with the non-equilibrium chemical model `FRECKLL`. Exploring a three-dimensional parameter space of metallicity, C/O ratio, and vertical mixing (K_{zz}), we generate synthetic spectra and compare them to observations to refine atmospheric constraints. Our best-fit model indicates high metallicity (266^{+291}_{-104} at 2σ) and a super-solar C/O ratio (C/O $\geq$ 2.1 at 2σ). Methane (CH_4) is robustly detected, while CO2 and other species remain uncertain due to spectral overlap and noise. The role of K_{zz} is unconstrained, but non-equilibrium models strongly outperform flat-line fits, confirming atmospheric features. Minor species, including potential prebiotic molecules, may exist at trace levels though likely obscured. These findings emphasize the necessity of non-equilibrium chemistry in interpreting exoplanetary spectra and suggest complex atmospheric processes on K2-18 b. Future high-resolution JWST and ELT observations will be essential to constrain minor species, assess aerosol formation, and evaluate the planet's potential habitability.

Keywords: exoplanets, atmospheres, chemistry, K2-18 b

1 Introduction

The detection of Earth-like habitable planets is limited by weak signals, but M-dwarf stars offer favorable conditions for studying smaller exoplanets such as sub-Neptunes, which are common yet absent from the Solar System (Fressin et al. 2013; Luger & Barnes 2015; Owen & Mohanty 2016; Van Eylen et al. 2018; Hardegree-Ullman et al. 2019; Cabot et al. 2024). Their H_2-rich atmospheres produce strong spectral features, making them promising for atmospheric characterization despite challenges posed by stellar activity (Scalo et al. 2007; Ricker et al. 2015; Shields et al. 2016; Rimmer et al. 2018).

K2-18 b, a temperate sub-Neptune in the habitable zone, has been characterized with HST (Tsiaras et al. 2019; Benneke et al. 2019) and JWST (Madhusudhan et al. 2023; Wogan et al. 2024; Schmidt et al. 2025). HST confirmed an H_2-dominated atmosphere but could not distinguish between H_2O and CH_4; JWST later revealed robust CH_4 and possible CO_2 (Madhusudhan et al. 2023). Disequilibrium chemistry models predicted CH_4 dominance (Blain et al. 2021) and more recent analyses favored higher CH_4 with uncertain CO_2 (Wogan et al. 2024; Schmidt et al. 2025). These findings underscore the importance of non-equilibrium chemistry, as also highlighted by SO_2 detection in WASP-39 b (Rustamkulov et al. 2023; Alderson et al. 2023; Tsai et al. 2023).

Atmospheric composition depends on metallicity, C/O ratio, and vertical mixing. Past studies constrained metallicity at 100-400$\times$ solar (Tsiaras et al. 2019; Benneke et al. 2019; Fortney et al. 2013), explored broad K_{zz} values (Bézard et al. 2022), and considered variable C/O ratios (Blain et al. 2021; Wogan et al. 2024; Schmidt et al. 2025).

This work aims to simultaneously explore metallicity, C/O, and K_{zz} for K2-18 b using the non-equilibrium model FRECKLL (Al-Refaie et al. 2024) with JWST data (Madhusudhan et al. 2023), to refine atmospheric constraints and assess the chemistry of minor species.

[1] LATMOS/IPSL, UVSQ Université Paris-Saclay, Sorbonne Université, CNRS, Guyancourt, France.
[2] Laboratoire d'astrophysique de Bordeaux, Univ. Bordeaux, CNRS, B18N, allée Geoffroy Saint-Hilaire, 33615 Pessac, France.
[3] Université Paris Cité and Univ Paris Est Creteil, CNRS, LISA, F-75013 Paris, France.
[4] ENS Paris-Saclay, Université Paris-Saclay, Gif-sur-Yvette, 91190, France.

2 Methods

The methodology combines non-equilibrium chemical modeling with observational data from JWST to constrain the atmospheric properties of K2-18 b.

First, we modeled the atmosphere using a three-dimensional parameter grid spanning metallicity, C/O ratio, and vertical mixing (K_{zz}). For each model, theoretical transmission spectra were computed and compared to JWST observations using χ^2 statistics.

We adopted the transit spectra from Madhusudhan et al. (2023), obtained with NIRISS SOSS and NIRSpec G395H (0.9-5.2 μm). A -41 ppm offset between the two instruments was accounted for. Model comparisons used native-resolution data, while lower-resolution spectra were used for visualization.

We performed a Bayesian equilibrium retrieval with `TauREx 3` (Al-Refaie et al. 2021), employing the `ACE` chemical model (Agúndez et al. 2012, 2020), identified as most suitable by Jaziri et al. (2024). We used ExoMol cross-sections (Yurchenko et al. 2011; Tennyson & Yurchenko 2012; Barton et al. 2013; Yurchenko et al. 2014; Barton et al. 2014; Chubb et al. 2021) for nine key species (e.g., H_2O, CH_4, CO_2, NH_3). Free parameters included cloud pressure, planetary radius, metallicity, and C/O ratio. The resulting fits were compared directly to non-equilibrium models.

We applied the 1D `FRECKLL` model (Al-Refaie et al. 2024), which solves continuity equations including ∼2000 reactions among ¿100 species, based on networks from Venot et al. (2012); Moses et al. (2011); Venot et al. (2020). Vertical mixing was parameterized with K_{zz}, and photolysis rates computed using MUSCLES GJ 436 version 2.2 stellar spectra (France et al. 2016; Youngblood et al. 2016; Loyd et al. 2016). Simulations explored metallicities (0.1-1000× solar), C/O ratios (0.1-100), and K_{zz} (10^5-10^{10} cm^2 s^{-1}). The temperature profile followed Blain et al. (2021). Cloud condensation was not included, but parallel fits excluded H_2O opacity to test C/O sensitivity.

Transmission spectra were generated with `TauREx 3` using `FRECKLL` outputs. Planet radius was retrieved to align model and data. Best fits were determined via χ^2 minimization, with confidence intervals defined in 1D and 2D parameter space. Results were compared against flat-line models to confirm the statistical significance of atmospheric features, following approaches by Blain et al. (2021); Wogan et al. (2024).

This framework provides estimates of K2-18 b's metallicity and C/O ratio, while constraining minor species abundances and assessing the preference for non-equilibrium chemistry over equilibrium scenarios.

3 Results and discussion

The best-fit values (on the model grid) are 280.7 for metallicity, 90.0 for the C/O ratio, and 10^6 cm^2,s^{-1} for Kzz, with a corresponding χ^2 of 4786.25.

3.1 Transmission spectra and species detection

The transmission spectra within 3σ of the best fit are shown in Figure 1, with the shaded area representing the uncertainty. The main spectral features are attributed to CH_4, CO_2, and CO, while secondary features from H_2O and NH_3 appear near 2 and 3,μm (Figure 2). Comparing the disequilibrium models to a flat-line retrieval (Figure 1) shows that the best disequilibrium model achieves a confidence level exceeding 4σ, confirming the robustness of the observed spectral features.

To accurately characterize K2-18,b's atmosphere, particularly under its specific temperature, irradiation, and vertical transport conditions, comprehensive chemical models including non-equilibrium processes are essential. While the atmosphere is likely chemically rich, retrievals assuming constant abundance profiles confirm only the presence of CH_4. The CH_4 and CO_2 detections with inferred abundances of ∼1% reported by Madhusudhan et al. (2023) are within 3σ of our best-fit model. CH_4 appears more abundant than CO_2, consistent with disequilibrium models (e.g., Wogan et al. 2024). CO2 abundances can drop as low as log10[CO_2] = -6.5 at 1 mbar, agreeing with Schmidt et al. (2025), who question the robustness of CO_2 detection.

Other species such as CO, H_2O, and C_2H_4 may reach a few percent in mixing ratios but remain undetected due to spectral masking by CH_4 or observational noise. NH3 can reach log10[NH_3] = -3.2 at 1 mbar, consistent with disequilibrium predictions, though its apparent absence in spectra may reflect limitations in sensitivity or nitrogen sequestration in deep magma oceans (Shorttle et al. 2024). Similarly, H_2O may be overestimated in our models due to the neglect of condensation processes. High-resolution ground-based spectroscopy, such as ANDES on the ELT, will likely be required to detect these hidden species.

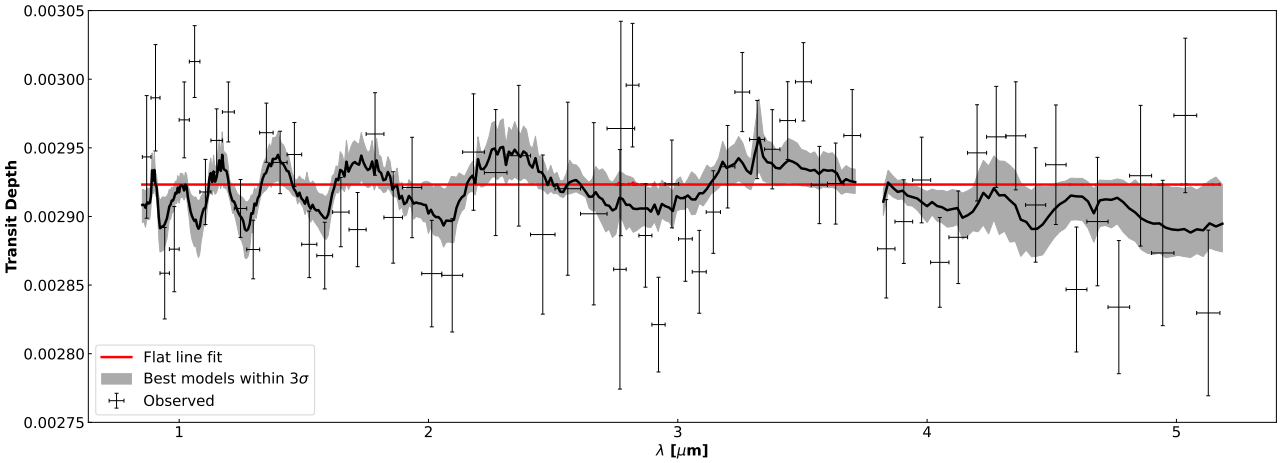

Fig. 1. Transit spectra of non-equilibrium 1D models at resolution 200, compared to K2-18 b observation (Madhusudhan et al. 2023) low-resolution representation with an offset of -41ppm between NIRISS and NIRSpec data. The solid gray line is the median value of the 3σ dispersion from the best fit represented with the shaded area. The red line is the best flat line retrieval.

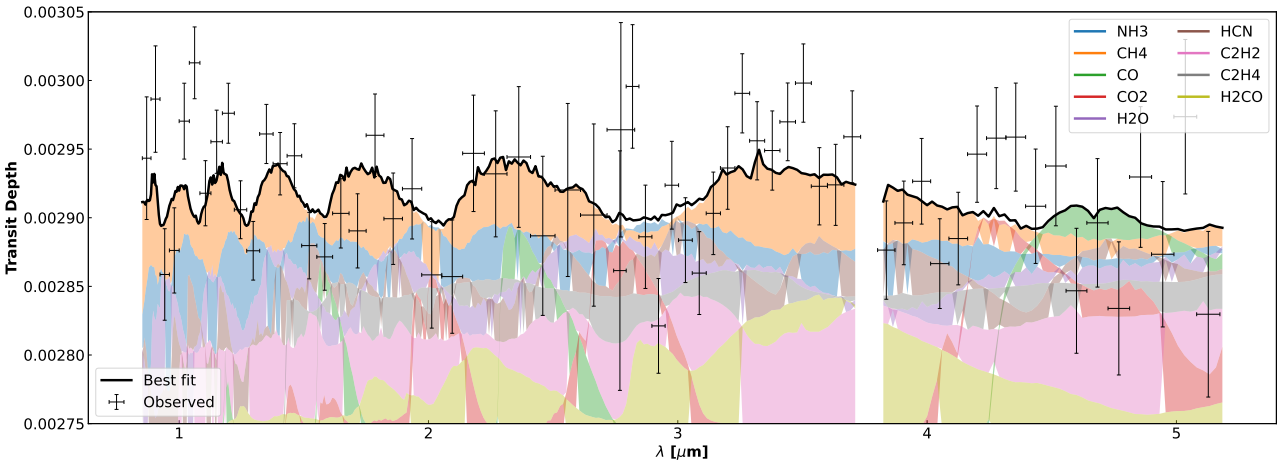

Fig. 2. Transit spectra of the best-fit non-equilibrium 1D model at resolution 200 (black solid line). This is the approximate best fit on the simulated grid of metallicity, C/O, and K_{zz}; the values are respectively 280.7, 90.0, and 10^6 $cm^2.s^{-1}$. They are compared to a K2-18 b observation (Madhusudhan et al. 2023) low-resolution representation with an offset of -41ppm between NIRISS and NIRSpec data. The contributions of the considered molecules are represented as shaded colors.

3.2 Equilibrium vs. non-equilibrium chemistry

The best-fit equilibrium model yields a metallicity of 71^{+58}_{-20} and a C/O ratio of $6.78^{+5.8}_{-2.0}$. Spectral features are dominated by CH_4 and CO_2, with little difference between equilibrium and non-equilibrium chemistry for CH_4. The best-fit equilibrium model has a slightly lower χ^2 ($\Delta\chi^2 = -2.0$) than the best non-equilibrium model, indicating a marginally better fit. Nevertheless, non-equilibrium chemistry significantly affects the abundances of H_2O, NH_3, and CO_2, though these remain below current detection limits.

3.3 Eddy diffusion coefficient

K_{zz} is not constrained. Reducing the 3D parameter space to 1D along metallicity and C/O shows χ^2 variations within 1σ of the best fit. Vertical transport significantly affects minor species but has little impact on major species such as CH4, explaining why Kzz remains unconstrained.

3.4 Metallicity and its bimodality

Metallicities $\lessapprox 100$ are statistically less significant than a flat line. The best fit corresponds to a metallicity of 280.7. A 2σ confidence interval derived from a polynomial fit gives 266^{+291}_{-104}, with a 3σ lower limit of $\geq$129.

Two regimes emerge:

C/O $\lessapprox$ 2: High metallicities ($\gtrsim$100) are favored, but uncertainties are large between 100-1000.

C/O $\gtrsim$ 2: Increasing C/O constrains metallicity to 205-356 at 1σ, consistent with Fortney et al. (2013).

The observed bimodality arises from exploring the full metallicity-C/O parameter space. Previous studies assuming solar C/O exclude only low metallicities, whereas high C/O reveals a distinct metallicity regime. Elevated metallicities flatten spectra, and in combination with high C/O, can lead to dominance of C_2H_4 over CH_4, which degrades the fit if too extreme.

3.5 C/O ratio

Low C/O ratios near solar ($0.55^{+0.130}_{-0.108}$ Lodders (2019)) are statistically insignificant. Our results favor a high C/O ratio, with a lower limit above 7.1 within 1σ, and ruling out the solar ratio at 3σ. Excluding H_2O opacity lowers 2σ and 3σ limits to 1.4 and 0.57, respectively.

3.6 Abundances

At 1 mbar, CH_4, CO_2, CO, H_2O, and C_2H_4 can reach up to 10% in mixing ratio. CO_2, H_2O, and C_2H_4 can fall below ppm levels, making detection uncertain. CH_4 remains the only strongly confirmed species, consistently above 1%. Oxidized species such as H_2CO, CH_3OH, and CH_3CHO may exist at ppm levels.

3.7 Challenges and observational limitations

Dominant CH_4 features obscure weaker species. Spectral mismatches at $\lambda \leq 2, \mu$m likely arise from aerosols, which affect the global spectral shape and can bias retrieved C/O ratios. Current S/N prevents confident detection of secondary species such as NH_3 and H_2O. High-resolution future observations are essential for probing minor constituents.

4 Conclusions

This study applied non-equilibrium chemical models using JWST observations and the `FRECKLL` framework to investigate the atmosphere of the temperate sub-Neptune K2-18,b. By exploring a wide range of metallicity, C/O ratio, and eddy diffusion (K_{zz}), the analysis reveals that K2-18,b likely has a high atmospheric metallicity (266^{+291}_{-104}) and a robust detection of CH_4, while CO_2 remains uncertain. Minor species such as CO, H_2O, and NH_3 are predicted to exist but are not directly detectable, highlighting the chemical complexity of the atmosphere and the necessity of non-equilibrium models to probe hidden species.

Constraining the C/O ratio remains challenging; a lower limit of 2.1 (2σ) is established, and hints of hazes may affect spectral features at wavelengths $\leq 2\mu$m. Variations in K_{zz} have minimal impact due to limited constraints from affected species.

Future observations with JWST and high-resolution ground-based spectroscopy (ELT/ANDES) are expected to improve detection of CO, CO_2, H_2O, and NH_3, enabling better constraints on elemental ratios and atmospheric non-equilibrium chemistry. Overall, K2-18 b's atmosphere is likely chemically rich and complex, emphasizing the need for advanced modeling and high-quality data to understand temperate sub-Neptunes and their potential habitability.

This project has received funding from the European Research Council (ERC) under the ERC OxyPlanets projects (grant agreement No. 101053033). This project acknowledges funding from the European Research Council (ERC) under the European Union's Horizon 2020 research and innovation programme (grant agreement No. 679030/WHIPLASH). O.V. acknowledges funding from the ANR through the project 'EXACT' (ANR-21-CE49-0008-01), as well as from the Centre National d'Études Spatiales (CNES).

References

Agúndez, M., Martínez, J. I., de Andres, P. L., Cernicharo, J., & Martín-Gago, J. A. 2020, A&A, 637, A59

Agúndez, M., Venot, O., Iro, N., et al. 2012, A&A, 548, A73

Al-Refaie, A. F., Changeat, Q., Waldmann, I. P., & Tinetti, G. 2021, ApJ, 917, 37

Al-Refaie, A. F., Venot, O., Changeat, Q., & Edwards, B. 2024, ApJ, 967, 132

Alderson, L., Wakeford, H. R., Alam, M. K., et al. 2023, Nature, 614, 664

Barton, E. J., Chiu, C., Golpayegani, S., et al. 2014, MNRAS, 442, 1821

Barton, E. J., Yurchenko, S. N., & Tennyson, J. 2013, MNRAS, 434, 1469

Benneke, B., Wong, I., Piaulet, C., et al. 2019, ApJ, 887, L14

Blain, D., Charnay, B., & Bézard, B. 2021, A&A, 646, A15

Bézard, B., Charnay, B., & Blain, D. 2022, Nature Astronomy, 6, 537

Cabot, S. H. C., Madhusudhan, N., Constantinou, S., et al. 2024

Chubb, K. L., Rocchetto, M., Yurchenko, S. N., et al. 2021, A&A, 646, A21

Fortney, J. J., Mordasini, C., Nettelmann, N., et al. 2013, ApJ, 775, 80

France, K., Loyd, R. O. P., Youngblood, A., et al. 2016, ApJ, 820, 89

Fressin, F., Torres, G., Charbonneau, D., et al. 2013, The Astrophysical Journal, 766, 81

Hardegree-Ullman, K. K., Cushing, M. C., Muirhead, P. S., & Christiansen, J. L. 2019, AJ, 158, 75

Jaziri, A. Y., Pluriel, W., Bocchieri, A., et al. 2024, A&A, 684, A25

Lodders, K. 2019, arXiv e-prints, arXiv:1912.00844

Loyd, R. O. P., France, K., Youngblood, A., et al. 2016, ApJ, 824, 102

Luger, R. & Barnes, R. 2015, Astrobiology, 15, 119

Madhusudhan, N., Sarkar, S., Constantinou, S., et al. 2023, ApJ, 956, L13

Moses, J. I., Visscher, C., Fortney, J. J., et al. 2011, ApJ, 737, 15

Owen, J. E. & Mohanty, S. 2016, MNRAS, 459, 4088

Ricker, G. R., Winn, J. N., Vanderspek, R., et al. 2015, Journal of Astronomical Telescopes, Instruments, and Systems, 1, 014003

Rimmer, P. B., Xu, J., Thompson, S. J., et al. 2018, Science Advances, 4

Rustamkulov, Z., Sing, D. K., Mukherjee, S., et al. 2023, Nature, 614, 659

Scalo, J., Kaltenegger, L., Segura, A., et al. 2007, Astrobiology, 7, 85, copyright: Copyright 2018 Elsevier B.V., All rights reserved.

Schmidt, S. P., MacDonald, R. J., Tsai, S.-M., et al. 2025, arXiv e-prints, arXiv:2501.18477

Shields, A. L., Ballard, S., & Johnson, J. A. 2016, Physics Reports, 663, 1, the habitability of planets orbiting M-dwarf stars

Shorttle, O., Jordan, S., Nicholls, H., Lichtenberg, T., & Bower, D. J. 2024, ApJ, 962, L8

Tennyson, J. & Yurchenko, S. N. 2012, MNRAS, 425, 21

Tsai, S.-M., Lee, E. K. H., Powell, D., et al. 2023, Nature, 617, 483

Tsiaras, A., Waldmann, I. P., Tinetti, G., Tennyson, J., & Yurchenko, S. N. 2019, Nature Astronomy, 3, 1086

Van Eylen, V., Agentoft, C., Lundkvist, M. S., et al. 2018, MNRAS, 479, 4786

Venot, O., Cavalié, T., Bounaceur, R., et al. 2020, A&A, 634, A78

Venot, O., Hébrard, E., Agúndez, M., et al. 2012, A&A, 546, A43

Wogan, N. F., Batalha, N. E., Zahnle, K. J., et al. 2024, ApJ, 963, L7

Youngblood, A., France, K., Loyd, R. O. P., et al. 2016, ApJ, 824, 101

Yurchenko, S. N., Barber, R. J., & Tennyson, J. 2011, MNRAS, 413, 1828

Yurchenko, S. N., Tennyson, J., & Bailey, J. e. a. 2014, Proceedings of the National Academy of Science, 111, 9379